

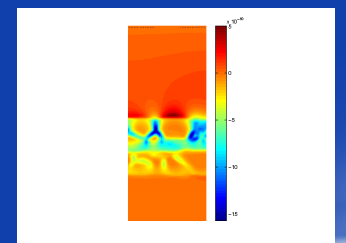
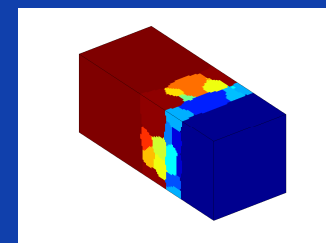
Phase-field modeling of microstructure evolution in multi-component alloys

Nele Moelans

*Department of Metallurgy and Materials Engineering (MTM)
K.U.Leuven, Belgium*

Liesbeth Vanherpe, Jeroen Heulens, Bert Rodiers

***COST MP0602 – Industrial
Seminar on Thermodynamics,
Bratislava, April 6, 2010***



- **Introduction: modeling of microstructure evolution**
- **Principles of phase field modeling**
- **Application examples**
 - Anisotropic grain growth
 - Precipitates on grain boundaries
 - Lead-free solder joints
 - Solidification
- **Summary**

Role of microstructures in materials science

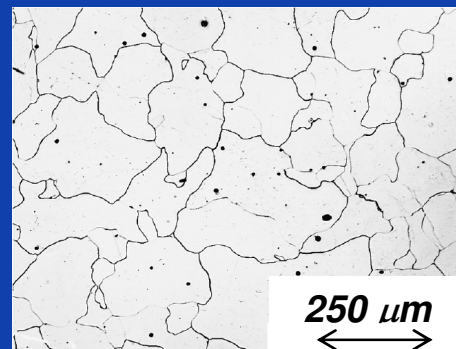
Chemical composition
+
*Temperature, pressure, cooling rate,
deformation, ...*



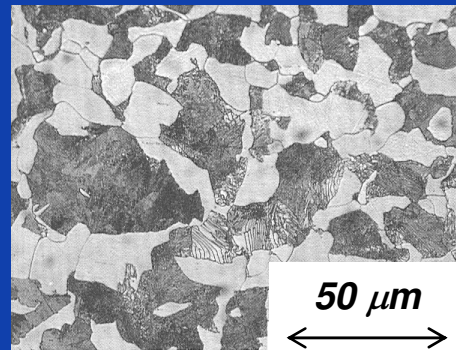
Microstructure
*Shape, size and orientation of the grains,
mutual distribution of the phases*



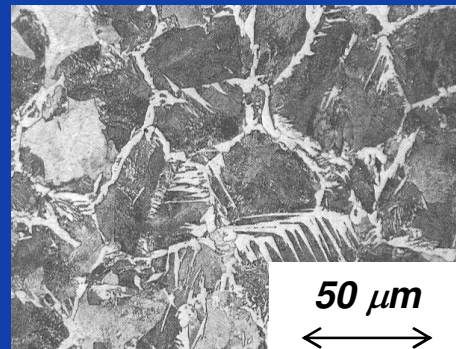
Material properties
*Strength, deformability,
hardness, toughness, fatigue...*



Low-C steel: wt%
 $C < 0.022$
Ferrite + small
carbides



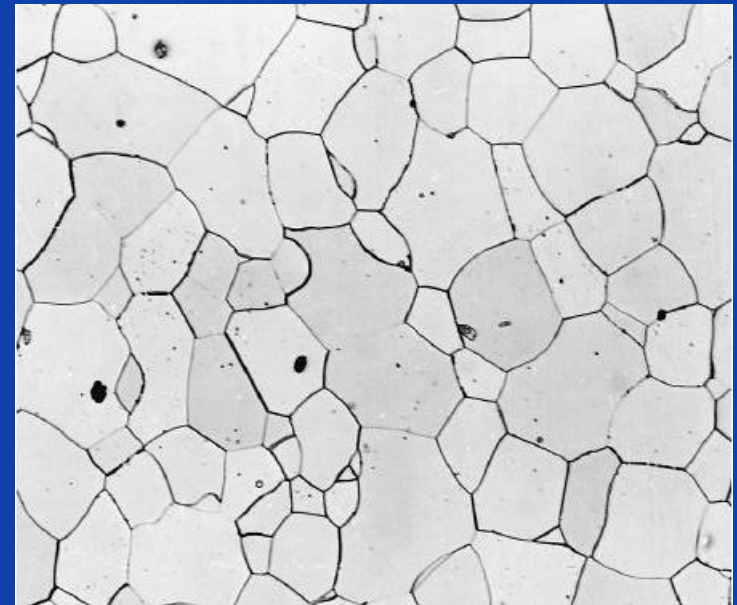
Steel: wt% $C =$
0.4, slow cooling
rate
Ferrite +
cementite



Steel: wt% $C =$
0.4, fast cooling
rate
Ferrite needles+
perlite

Microstructure evolution in multi-component alloys

- Connected grain structures
- Complex morphologies
- Concurrent processes
 - Solidification - grain growth - Ostwald ripening – diffusion - phase growth
- Materials' properties are largely related to microstructure
 - Material development
 - Reliability



Low C-steel, ferritic grain structure

Microstructure evolution in multi-component alloys

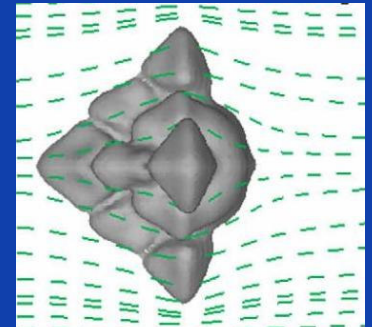
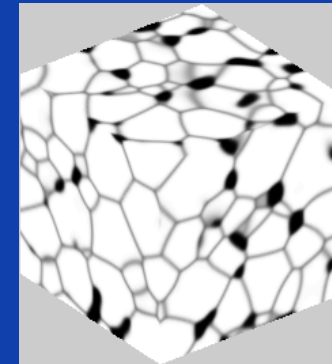
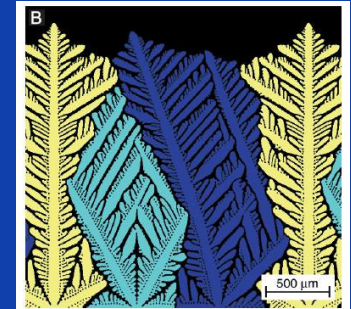
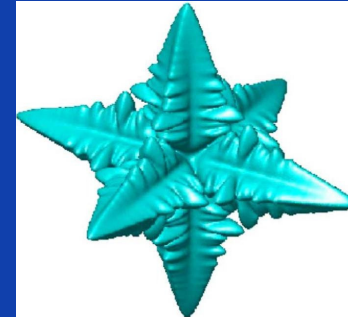
- **High complexity**
 - Anisotropy, segregation, solute drag, second-phase precipitates, pipe diffusion, mutual distribution of phases, ...
 - Many material properties: Crystal structure, Gibbs energy, diffusion coefficient of different phases? Structure, energy, mobility of grain boundaries?
 - Evolution connected grain structure ?
 - → Mesoscale simulations
- **Importance**
 - Material development: heat treatment, alloying
 - Reliability

Strength

- Complex shapes
- Multi-grain, multi-phase structures
- Thermodynamic driving forces

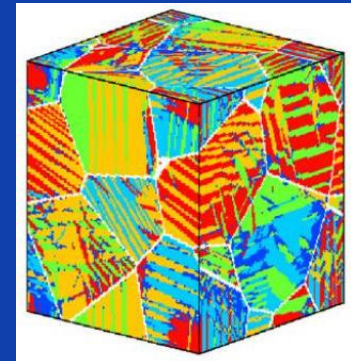
$$F = F_{chem} + F_{int} + F_{elast} + F_{magn} + \dots$$

- Multi-component
- Transport equations
 - Mass and heat diffusion/convection



Difficulties

- Implementation for realistic length scales
- Parameter choice

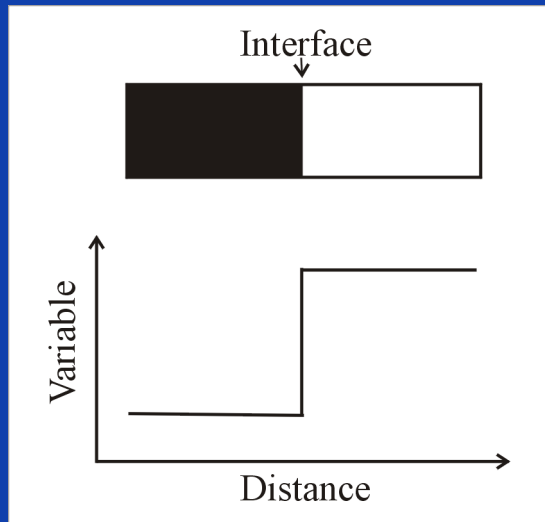


Principles of phase field modeling

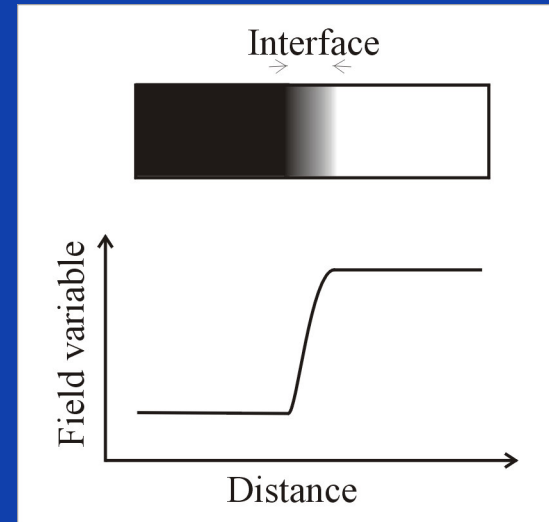
- Diffuse interface concept
- Phase field variables
- Thermodynamic free energy functional
- Evolution equations
- Parameter assessment
- Numerical implementation

Diffuse-interface description

- **Sharp interface**



- **Diffuse interface**



- **Discontinuous variation in properties**
- **Requires tracking of the interfaces**
- **Simplified grain morphologies**

- **Continuous variation in properties**
- **Interfaces implicitly given by local variations in phase-field variables**
- **Complex grain morphologies**

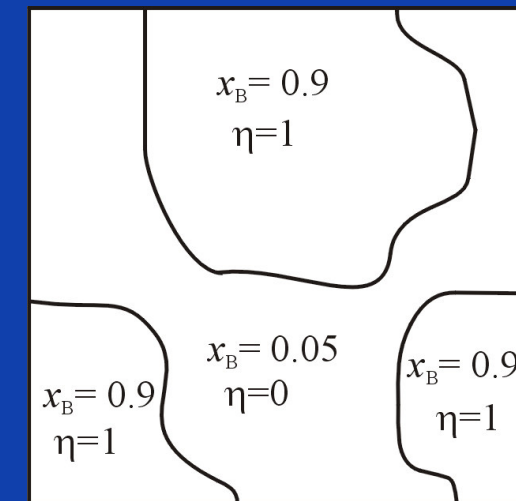
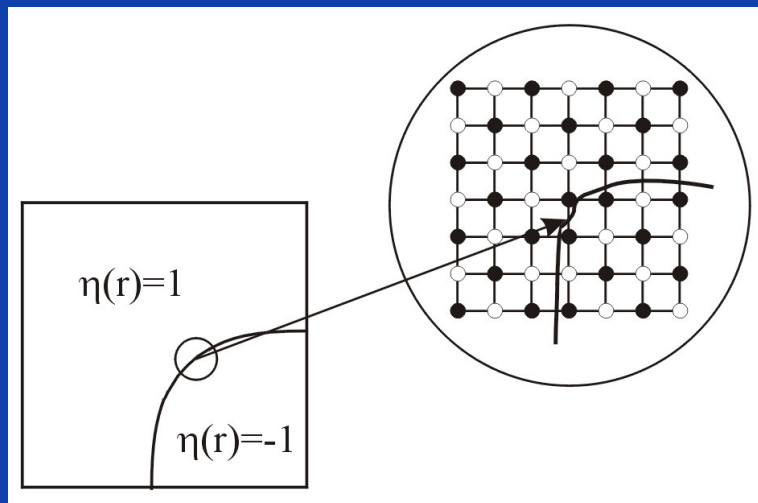
- *Diffuse interface approach* (van der Waals, Cahn-Hilliard (1958), Ginzburg-Landau (1950))
- Microstructure evolution started \pm 20 years ago

Representation of microstructures

- Phase-field variables: continuous functions in space and time

- Local composition $x_B(\vec{r}, t), c_B(\vec{r}, t)$

- Local structure and orientation $\eta(\vec{r}, t)$
 $\phi(r, t)$



Binary alloy A-B

- Phase α : $\eta = 0$
- Phase β : $\eta = 1$

- Free energy functional

$$F = F_{bulk} + F_{surface} = \int_V f_0(x_i, \eta_k, T) + \frac{K}{2} \sum_{k=1}^p (\nabla \eta_k)^2 + \frac{\varepsilon}{2} \sum_{i=1}^C (\nabla x_i)^2 dV$$

Homogeneous free energy
(chemical, elastic, ...)

Gradient free energy
(→ diffuse interfaces)

- Evolution of field variables

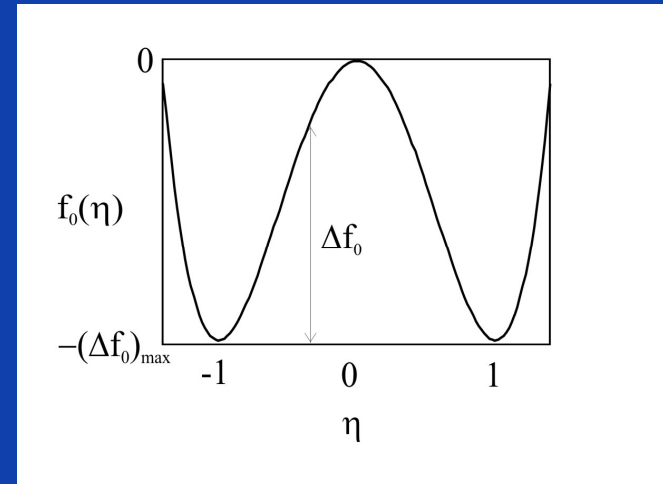
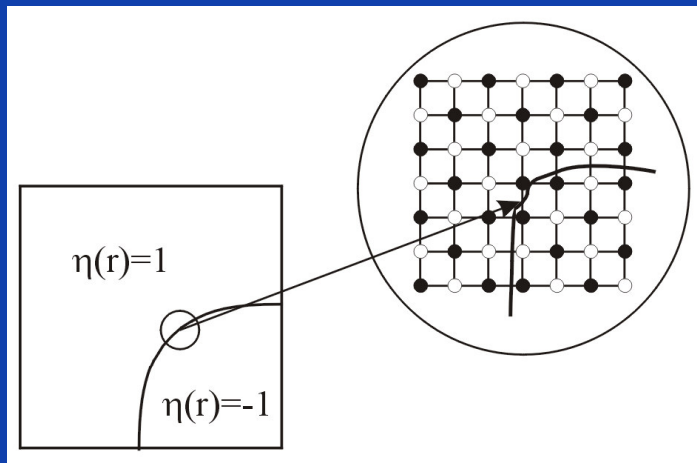
- Non-conserved field variables (→ Interface movement)

$$\frac{\partial \eta_k(\vec{r}, t)}{\partial t} = -L \frac{\partial F(x_1, \dots, x_C, \eta_1, \dots, \eta_p)}{\partial \eta_k(\vec{r}, t)} \quad (+\xi(\vec{r}, t))$$

- Conserved composition fields (→ Mass diffusion)

$$\frac{1}{V_m} \frac{\partial x_i(\vec{r}, t)}{\partial t} = \vec{\nabla} M \cdot \vec{\nabla} \frac{\partial F(x_1, \dots, x_C, \eta_1, \dots, \eta_p)}{\partial x_i(\vec{r}, t)} \quad (+\xi(\vec{r}, t))$$

- **Anti-phase boundary**



Boundary energy: $\propto \sqrt{\kappa(\Delta f_0)_{\max}}$

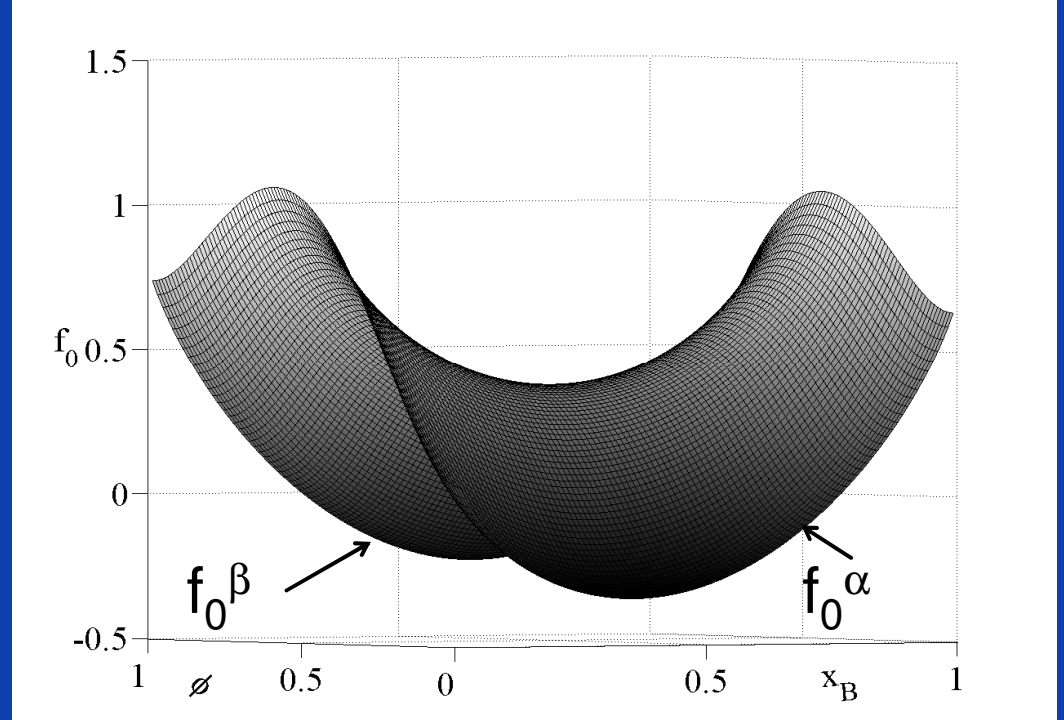
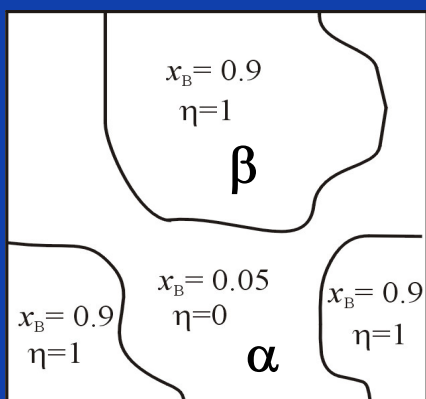
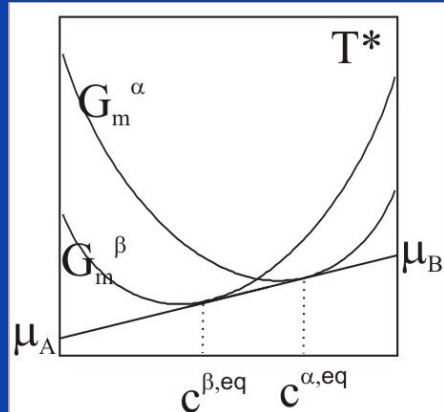
Boundary width: $\propto \sqrt{\frac{\kappa}{(\Delta f_0)_{\max}}}$

Boundary velocity: $\propto \kappa L$

$$f_0 = 4(\Delta f_0)_{\max} \left(\frac{\eta^4}{4} - \frac{\eta^2}{2} \right)$$

Homogeneous free energy

- **Binary two-phase system**

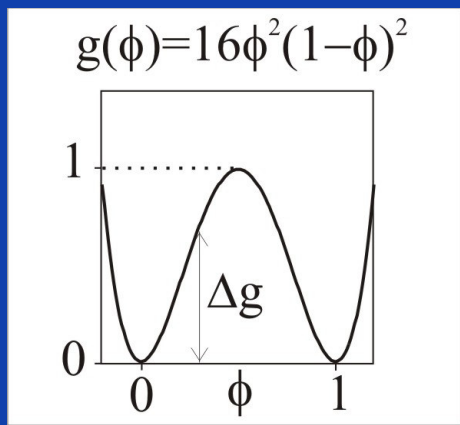
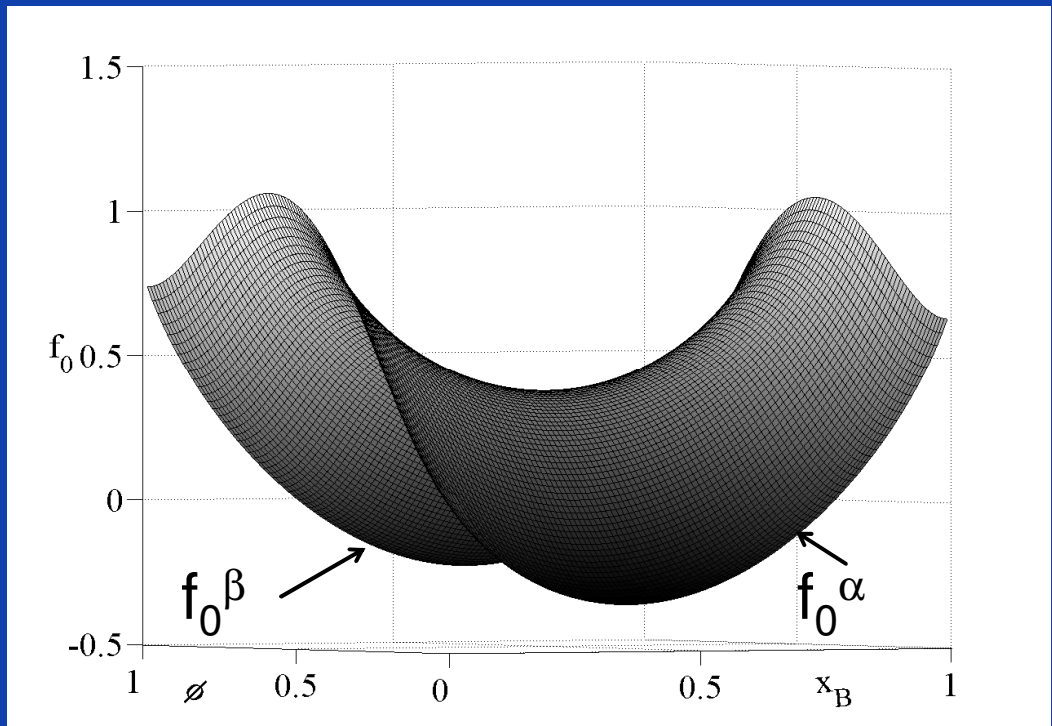
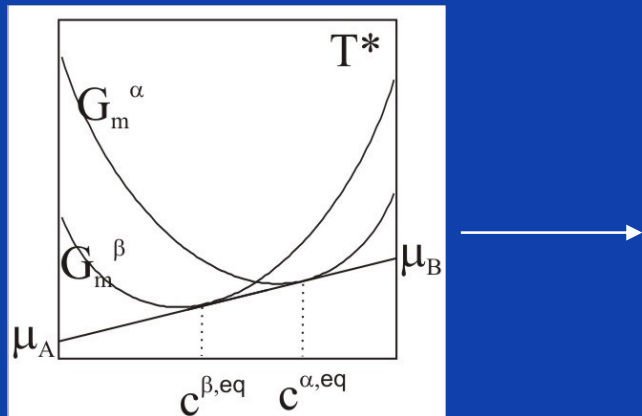


$$f_0 = h(\phi) f^\beta(c, T) + [1 - h(\phi)] f^\alpha(c, T) + \omega g(\phi)$$

$$\text{with } f^\alpha(c, T) = \frac{G_m^\alpha}{V_m}, \quad f^\beta(c, T) = \frac{G_m^\beta}{V_m} \quad (\text{CALPHAD})$$

Homogeneous free energy

- Binary two-phase system

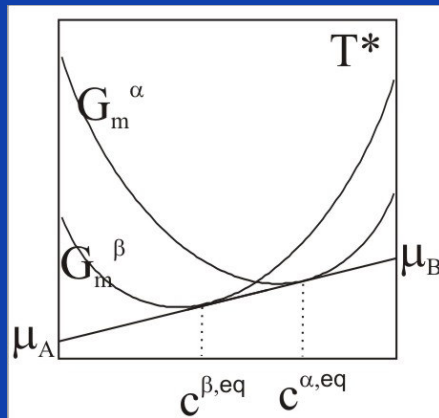


$$f_0 = h(\phi)f^\beta(c, T) + [1 - h(\phi)]f^\alpha(c, T) + \omega g(\phi)$$

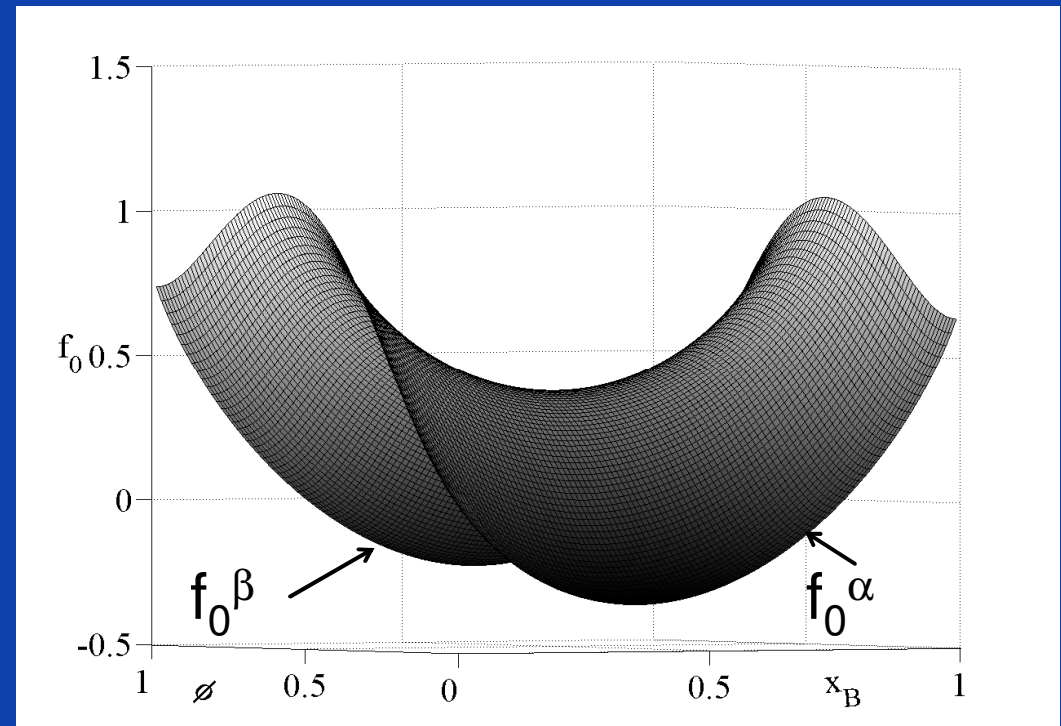
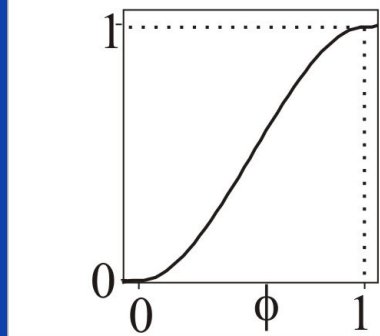
Double well function

Homogeneous free energy

- Binary two-phase system



$$h(\phi) = \phi^3(10 - 15\phi + 6\phi^2)$$

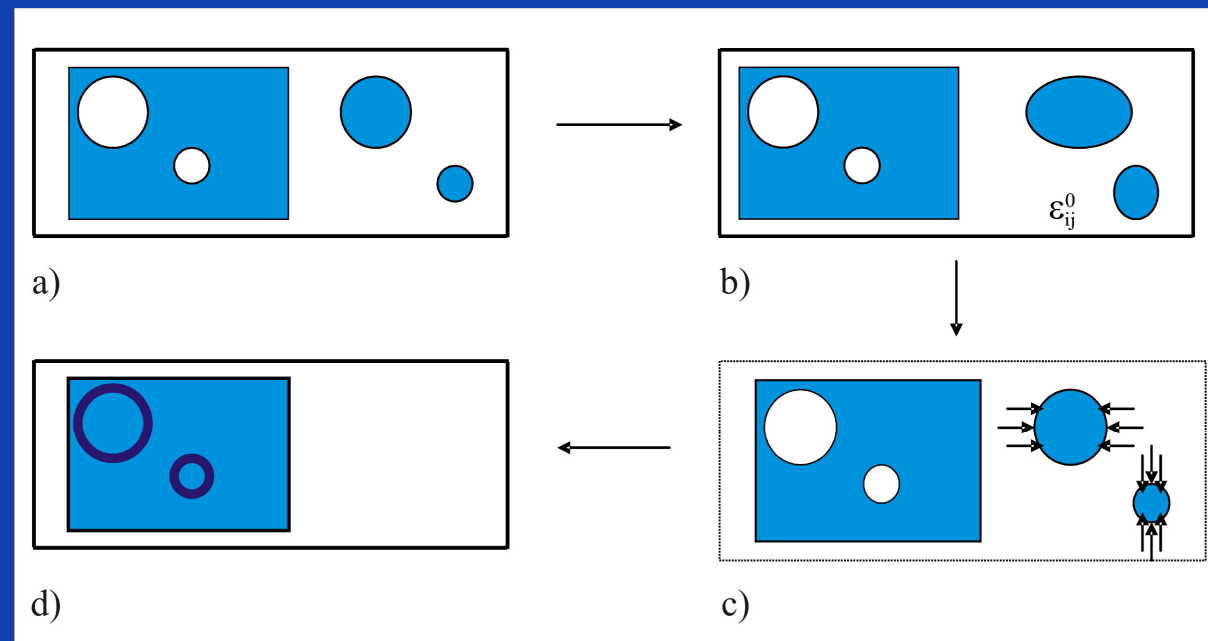


$$f_0 = h(\phi) f^\beta(c, T) + [1 - h(\phi)] f^\alpha(c, T) + \omega g(\phi)$$

Interpolation function

Effect of elastic stresses and strain

- Coupling with micro-elasticity theory → $F = F_{chem} + F_{int} + F_{elast}$
 - Effect of transformation and thermal strains, applied stress/strain
 - Martensitic transformation, precipitate growth



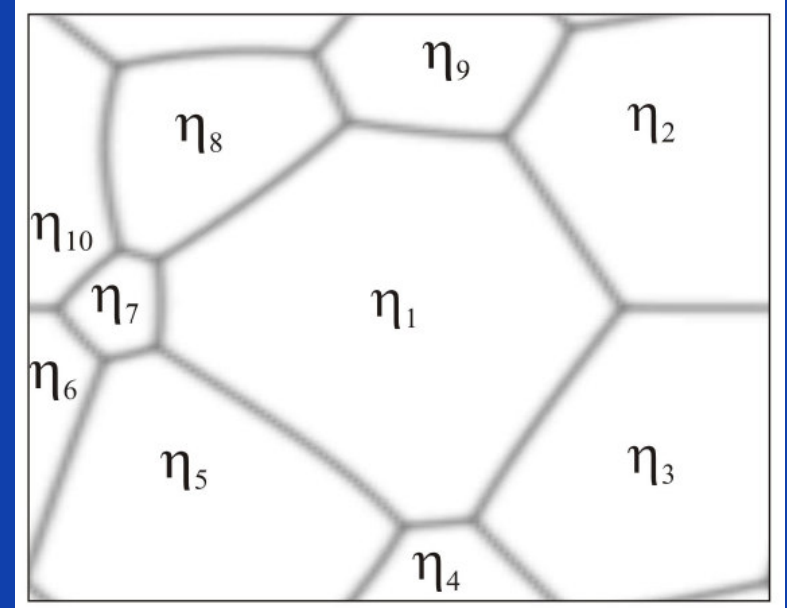
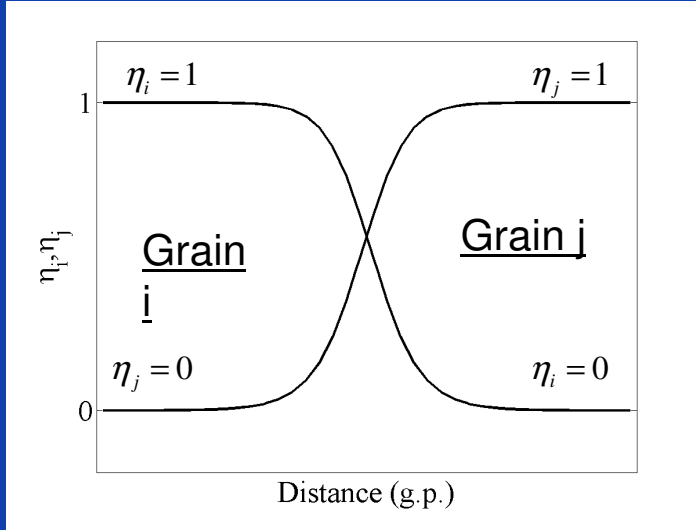
Polycrystalline structures

- **Polycrystalline microstructure**

$$\eta_1, \eta_2, \dots, \eta_i(\vec{r}, t), \dots, \eta_p$$

- **Grain i of matrix-phase**

$$(\eta_1, \eta_2, \dots, \eta_i, \dots, \eta_p) = (0, 0, \dots, 1, \dots, 0)$$



- **Free energy functional**

$$F = F_{surface} = \int_V f_0(\eta_1, \eta_2, \dots, \eta_p) + \frac{\kappa}{2} \sum_{k=1}^p (\nabla \eta_k)^2 dV$$

Multi-phase and multi-component alloys

- **Phase field variables:**

- **Grains**

$$\eta_{\alpha 1}, \eta_{\alpha 2}, \dots, \eta_{\alpha i}(\vec{r}, t), \dots,$$

$$\eta_{\beta 1}, \eta_{\beta 2}, \dots, \eta_p$$

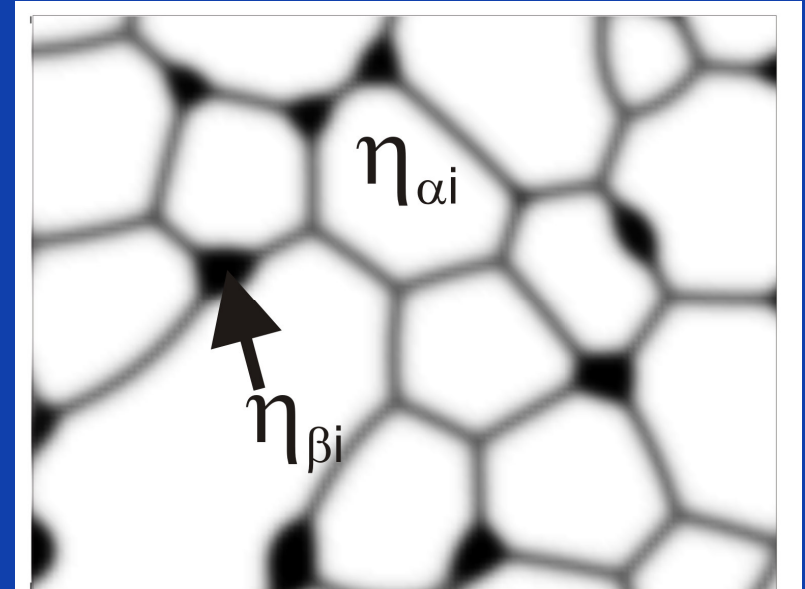
- **Composition**

$$x_A, x_B(\vec{r}, t), \dots, x_{C-1}$$

- **Free energy functional**

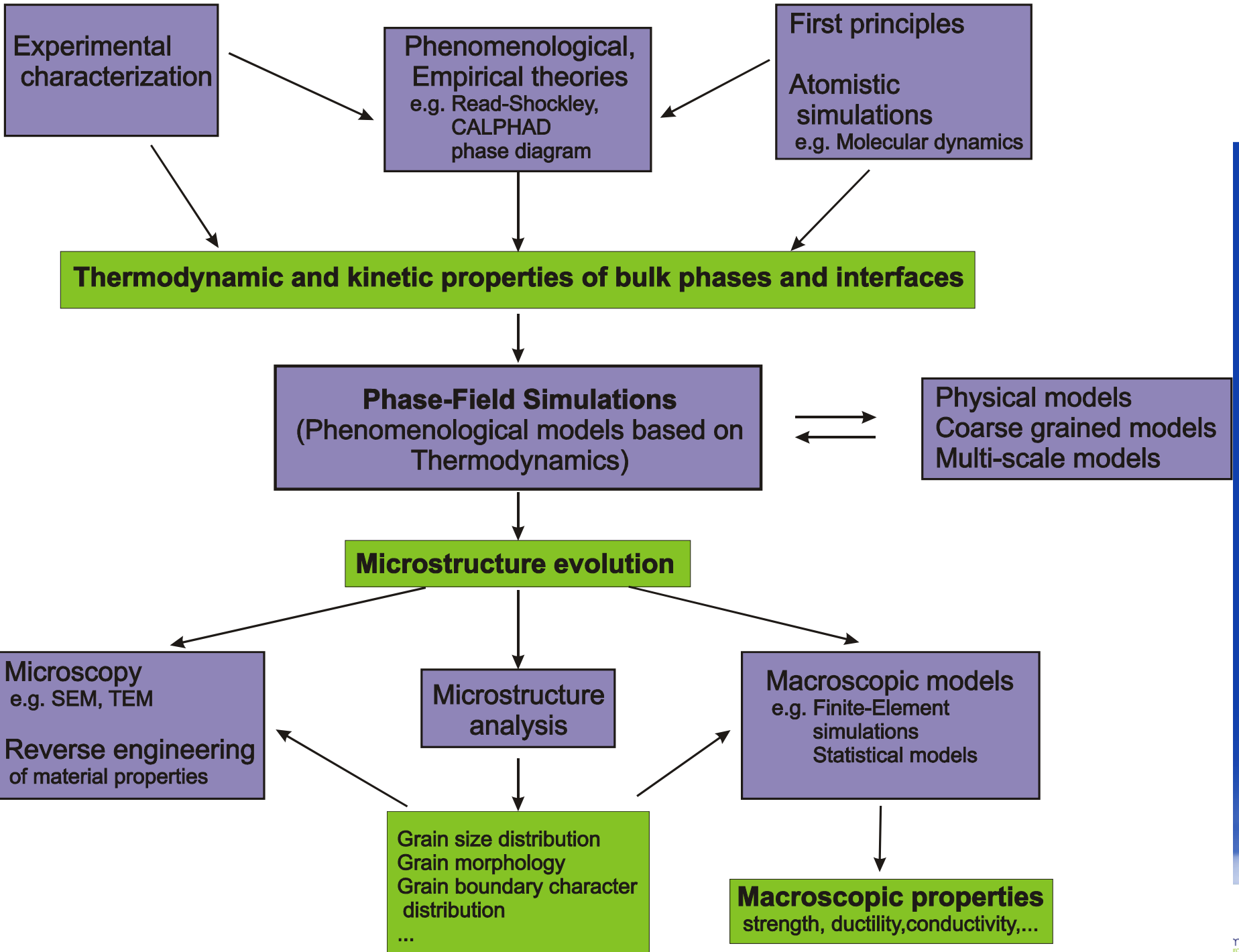
$$f_{bulk}(x_k, \eta_{\rho i}) = \sum_{\rho} h_{\rho}(\eta_{\rho i}) f^{\rho}(x_k^{\rho})$$

$$= \sum_{\rho} h_{\rho}(\eta_{\rho i}) \frac{G_m^{\rho}(x_k^{\rho})}{V_m}$$



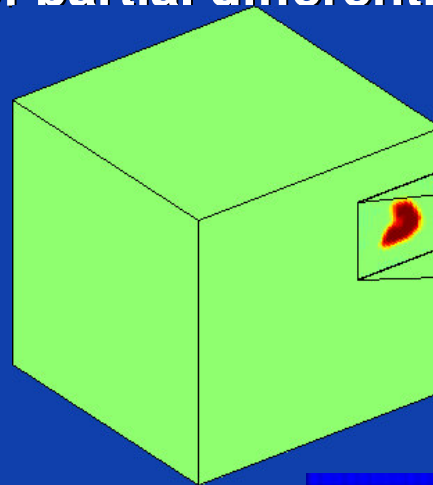
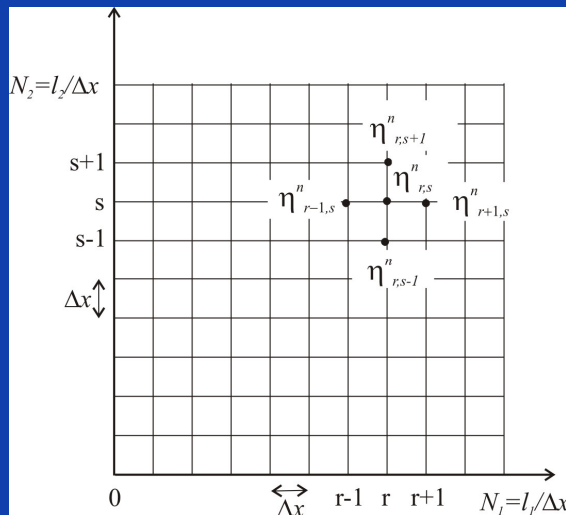
2 phase polycrystalline structure

- Different kinds of input data (calculated and/or measured)
 - Phase stabilities, phase diagram information
 - CALPHAD ← (ab-initio, experiments)
 - Interfacial energy and mobility
 - ab-initio, (MD, MC ← ab-initio), experimental
 - Elastic properties, crystal structure, lattice parameters
 - ab-initio, experimental
 - Atomic diffusion mobilities
 - CALPHAD ← ((MC ← ab-initio), experimental)
- Orientation and composition dependence
 - Anisotropy, segregation, solute drag

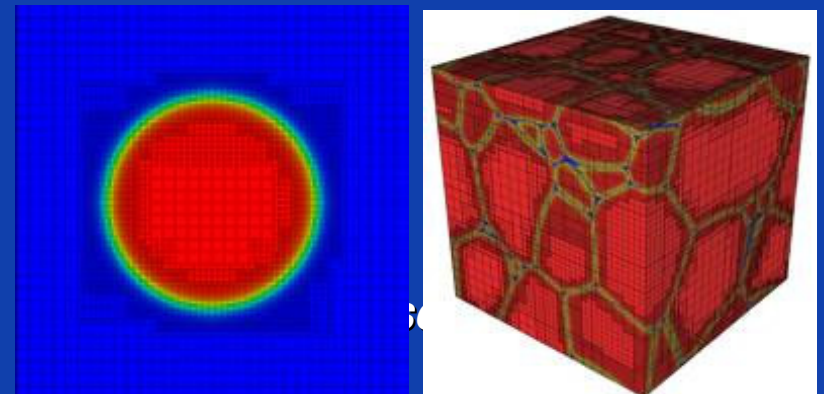


Quantitative aspects

- Numerical solution of partial differential equations



- **Bounding box algortihm**
 - Sparse data structure
 - Object oriented C++
- (L. Vanherpe et al., K.U.Leuven)



- **Discretization (Finite differences, finite elements, Fourier-spectral method)**

MICRESS, commercial software for phase-field coupled with CALPHAD

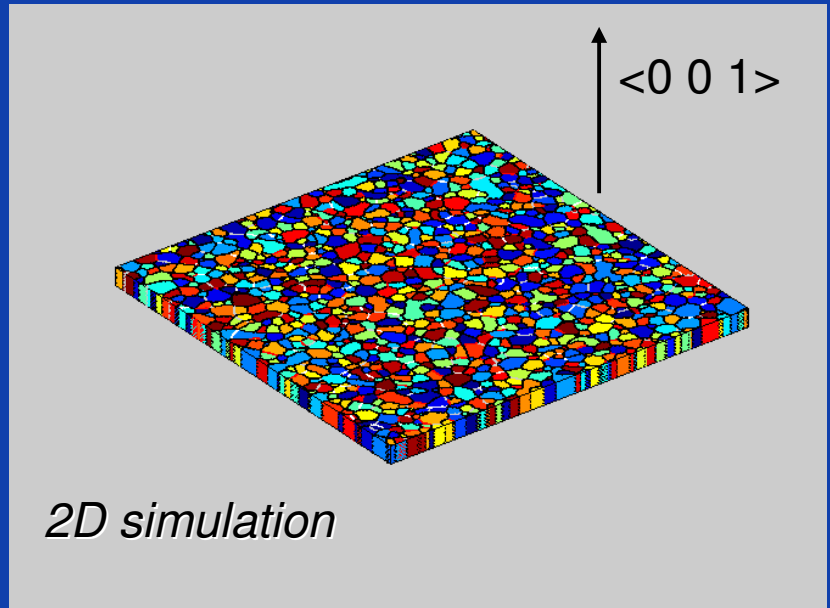
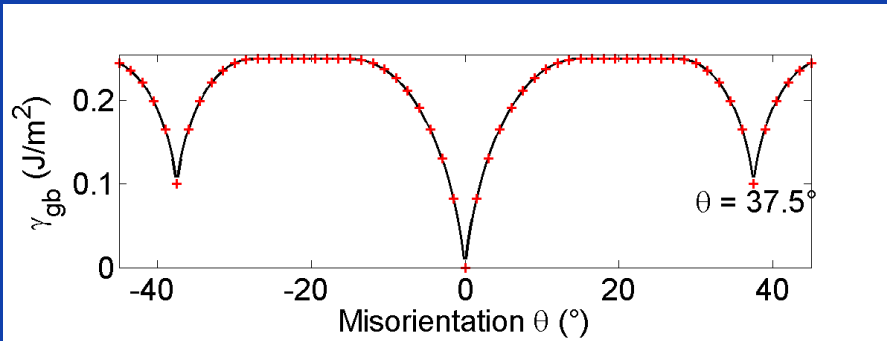
- **Adaptive meshing (M. Dorr et al. AMPE, LLNL)**

Examples of applications

- **Anisotropic grain growth**
- **Precipitates on grain boundaries**
- **Lead-free solder systems**
- **Solidification**

Columnar films with fiber texture

- **Grain boundary energy:**
 - Fourfold symmetry
 - Extra cusp at $\theta = 37.5^\circ$
 - Read-shockley

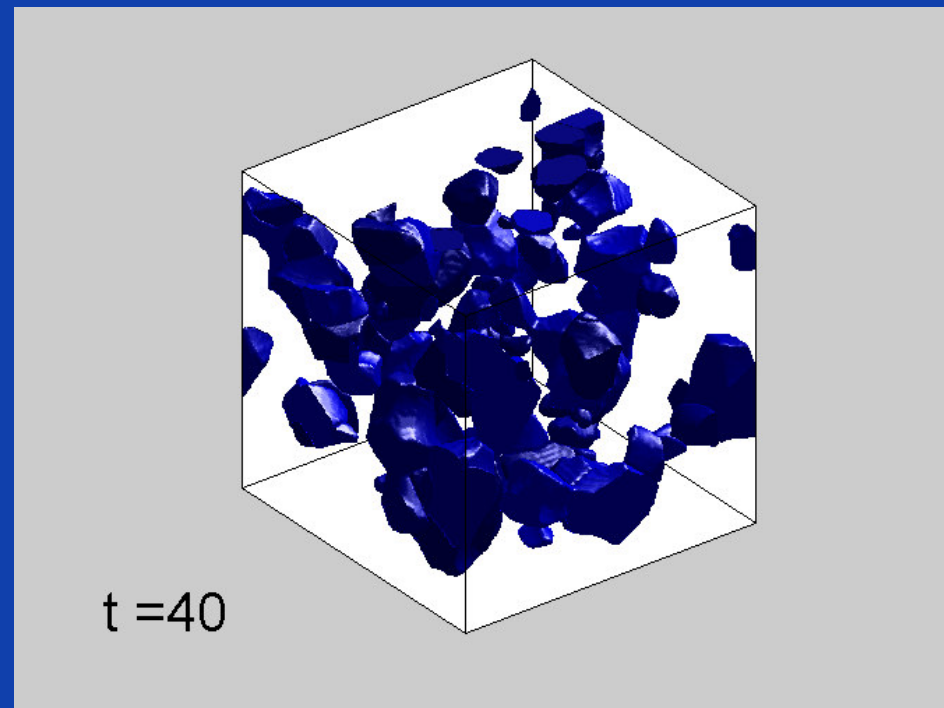


- **Discrete orientations**
 $\eta_1, \eta_2, \dots, \eta_i(\vec{r}, t), \dots, \eta_{60} \Rightarrow \Delta\theta = 1.5^\circ$
- **Constant mobility**
- **Initially random grain orientation and grain boundary type distributions**

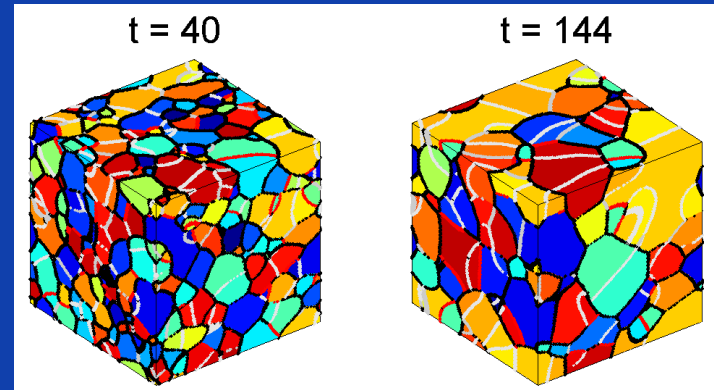
*White: $\theta = 1.5^\circ$
 Gray: $\theta = 3^\circ$
 Red: $\theta = 37.5^\circ$
 Black: $\theta > 3^\circ, \theta \neq 37.5^\circ$*

In collaboration with F. Spaepen, School of Engineering and Applied Sciences, Harvard University

3D simulations for wires with fiber texture



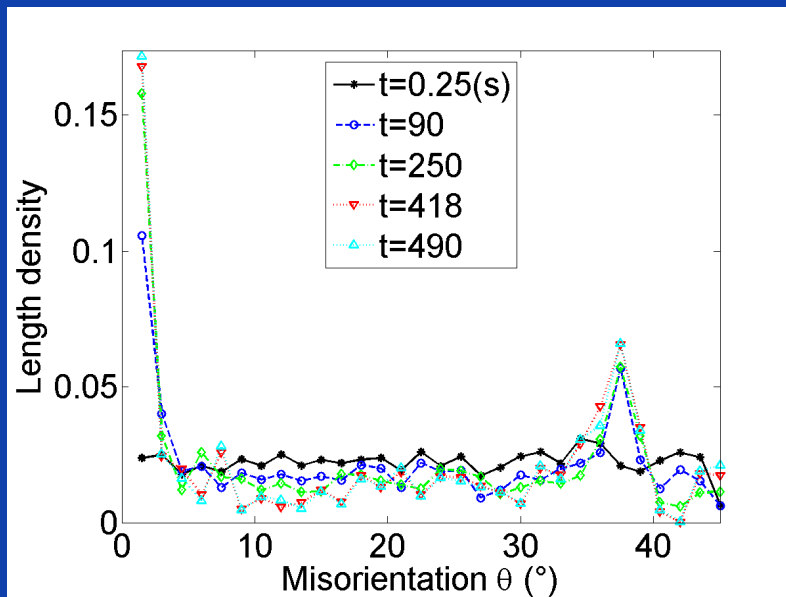
$t = 40$



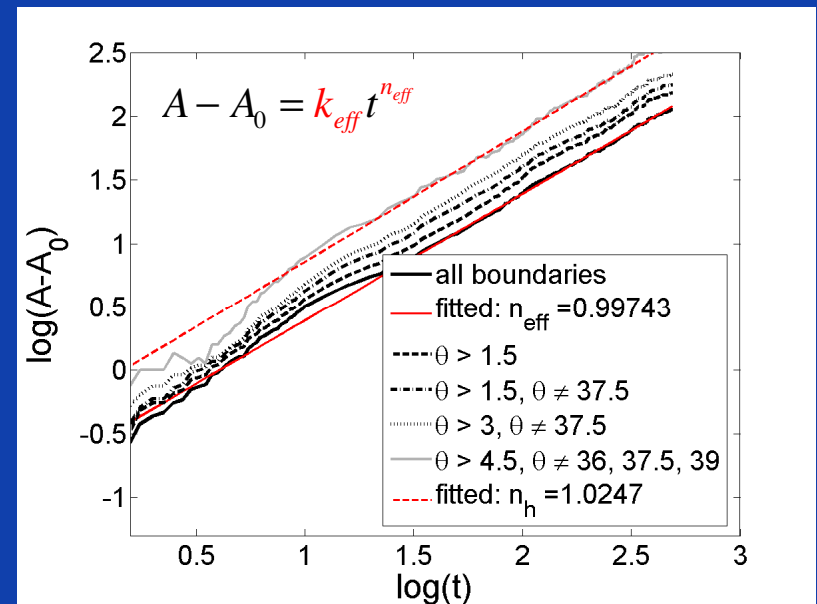
$$\vartheta < 6^\circ$$

Microstructure analysis: films

- Misorientation distribution function (MDF)



- Evolution mean grain area



- Evolution towards steady-state regime
→ Simple mean field models

$$n_{eff} = \frac{kt}{A_h(0) + kt} \rightarrow 1, t \rightarrow \infty$$

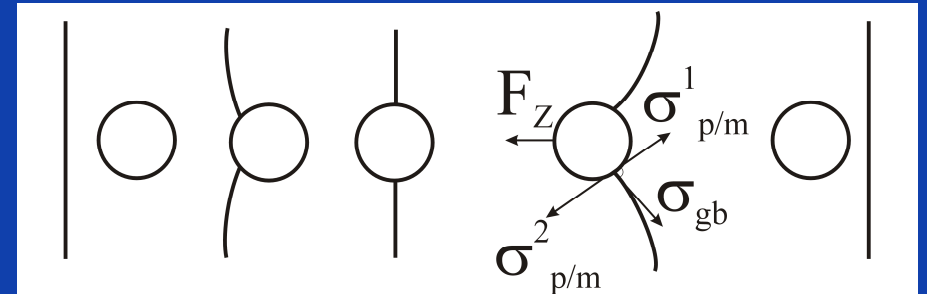
$$k_{eff} = \frac{dA_{eff}}{dt} = \frac{k}{1 + N'/N}$$

Examples of applications

- Anisotropic grain growth
- Precipitates on grain boundaries
- Lead-free solder systems
- Solidification

Zener pinning

- Mechanism for controlling grain size
 - E.g. NbC, AlN, TiN,... in HSLA-steels
 - Nano-grain structures

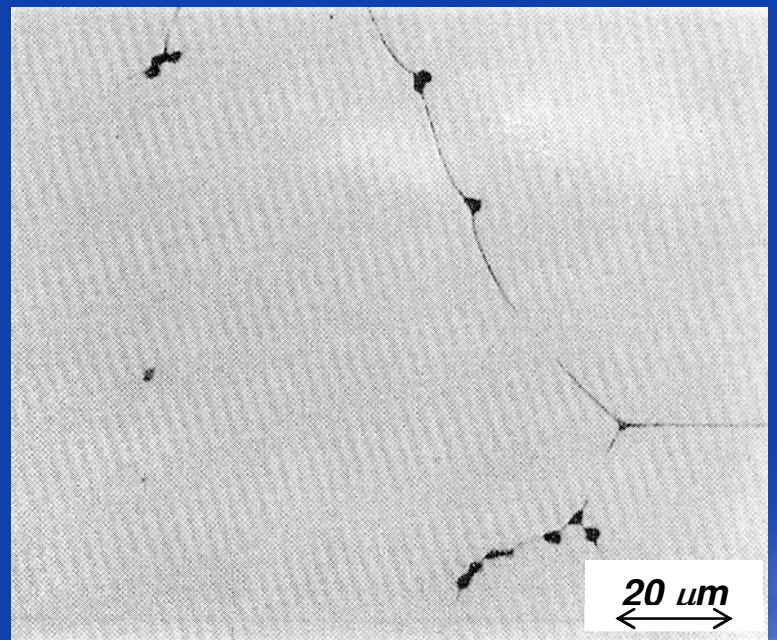


- Zener relation for limiting grain size

$$\frac{\bar{R}_{\text{lim}}}{r} = K \frac{1}{f_V^b}$$

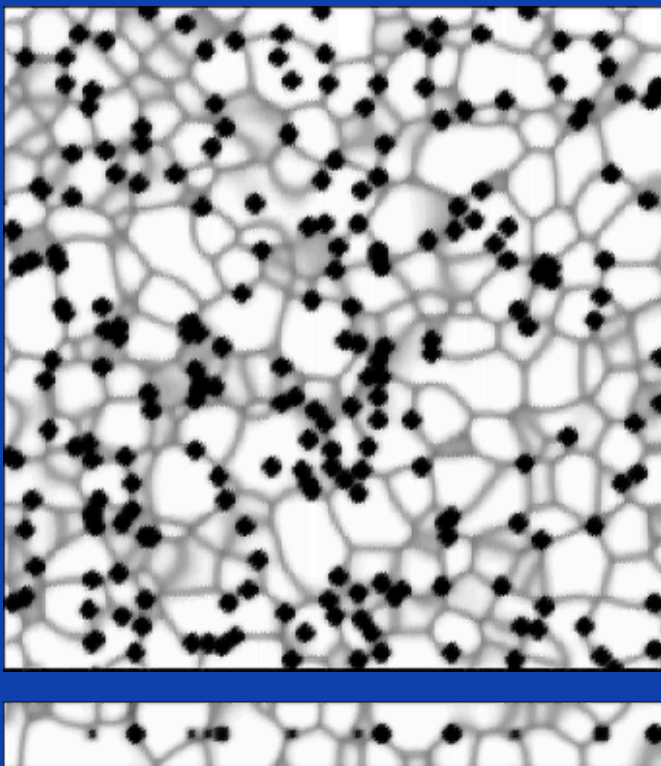
- Influence of
 - Shape of the particle
 - Interfacial properties of particles
 - Initial distribution
 - Evolution particles

Fe-0.09 to 0.53 w%
C-0.02 w% P with
Ce₂O₃ inclusions
(PhD. M. Guo)



Simulation results: Al thin films

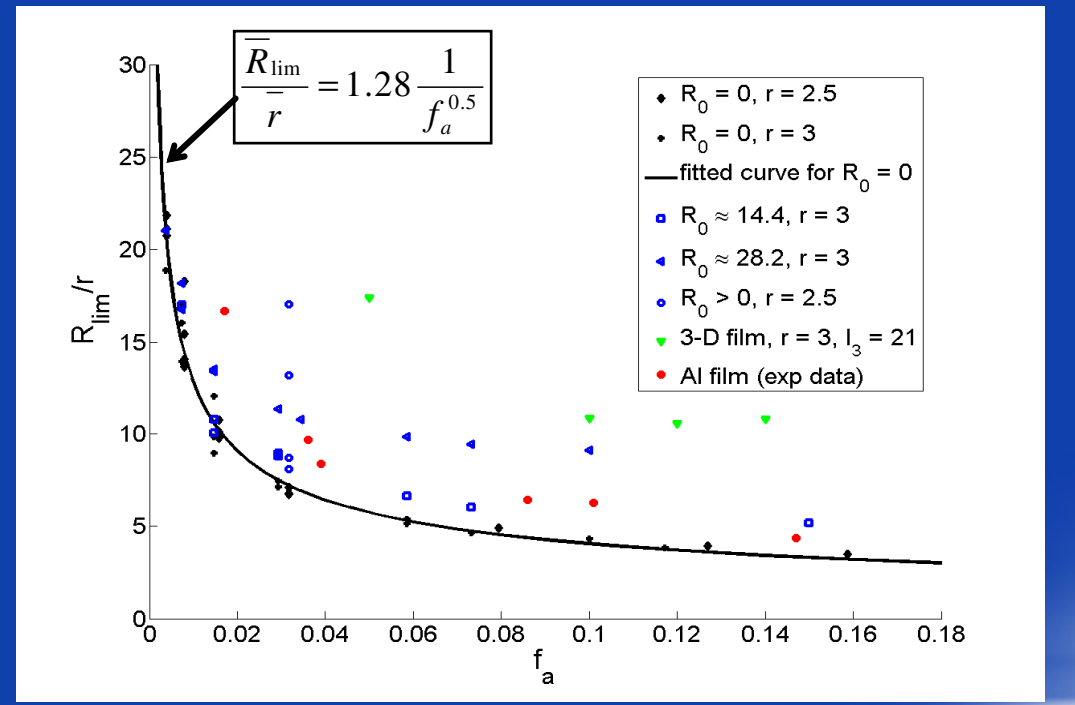
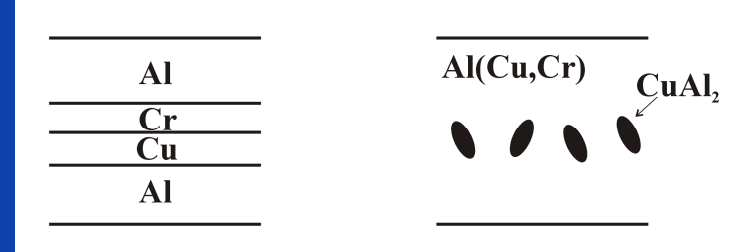
- Thin films with CuAl₂ - precipitates



$$r = 3, f_a = 0.12, l_3 = 21$$

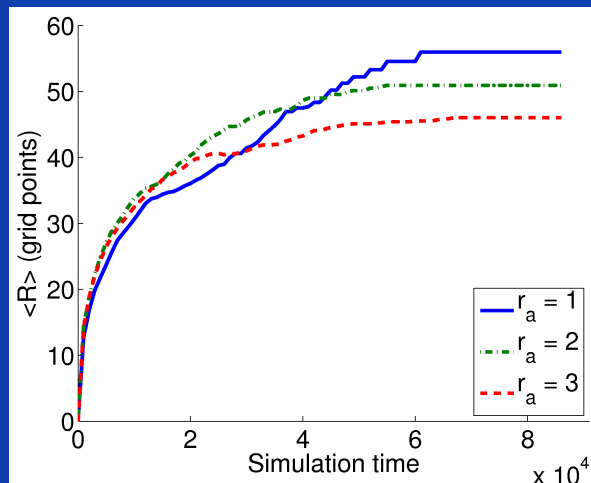
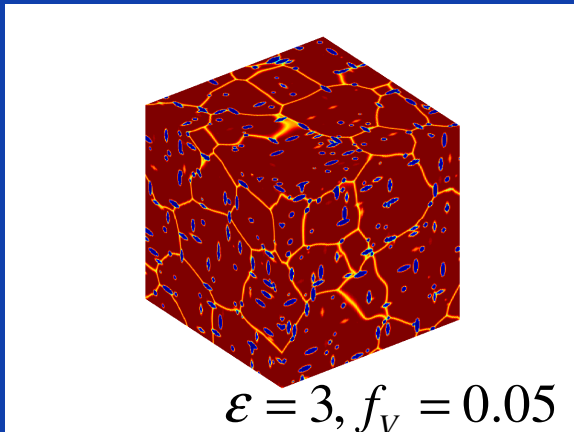
(exp from H.P. Longworth and C.V. Thompson)

Film preparation



Simulation results: effect of particle shape and coarsening

- Ellipsoid particles

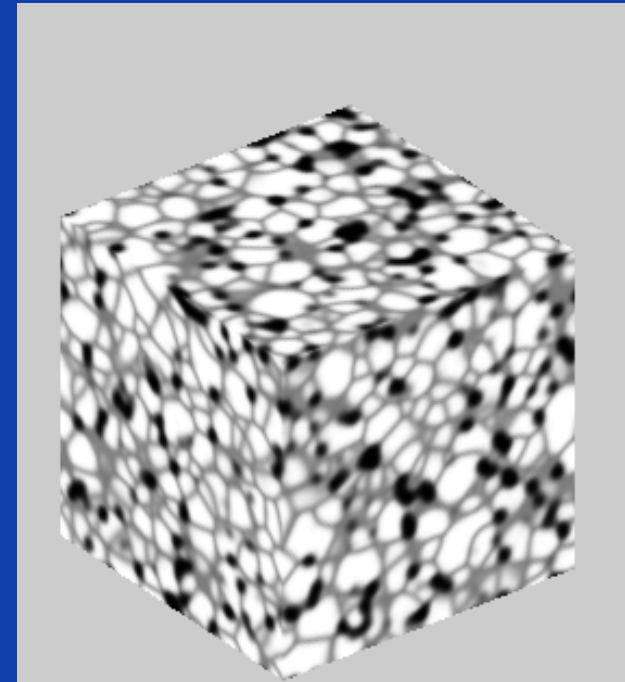


Modified Zener relation

$$\frac{\bar{R}_{\lim}}{s} = K \frac{r_a}{1 + ar_a} \frac{1}{f_V^b}$$

$$K = 3.7, b = 1, a = 3.1$$

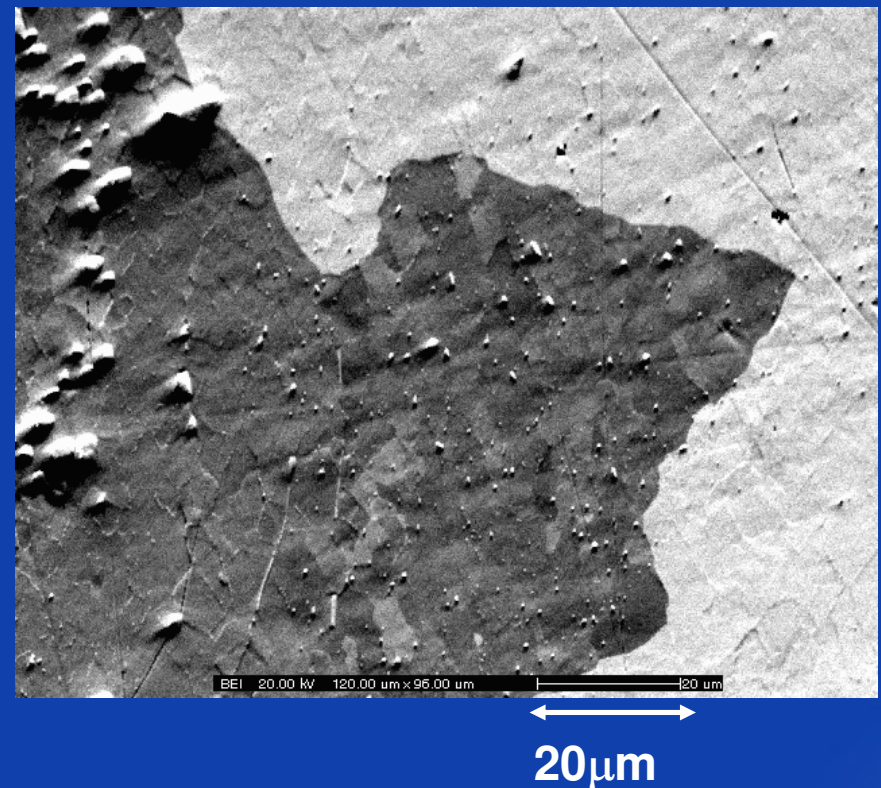
- Evolving particles



L. Vanherpe, K.U. Leuven

Jerky motion during recrystallization in Al-Mn alloy

- In-situ EBSD observation of recrystallization in AA3103 at 400 °C
 - CamScan X500 Crystal Probe FEGSEM
- Jerky grain boundary motion
 - Stopping time: 15-25 s
 - Pinning by second-phase precipitates
 - $\text{Al}_6(\text{Fe,Mn})$, $\alpha\text{-Al}_{12}(\text{Fe,Mn})_3\text{Si}$
- Added to phase field model
 - Grain boundary diffusion
 - Driving force for recrystallization



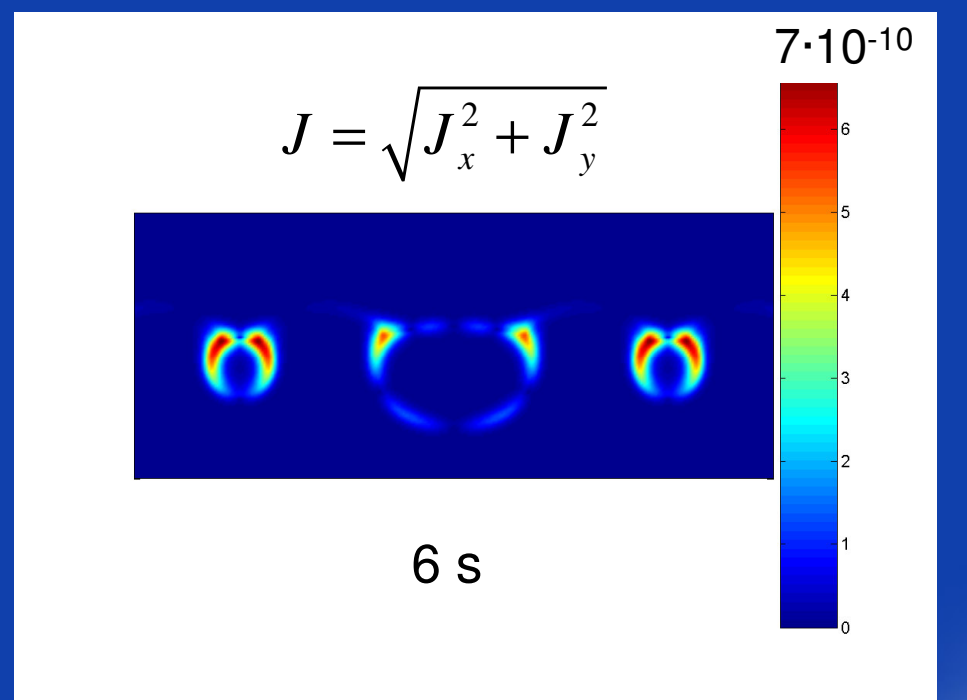
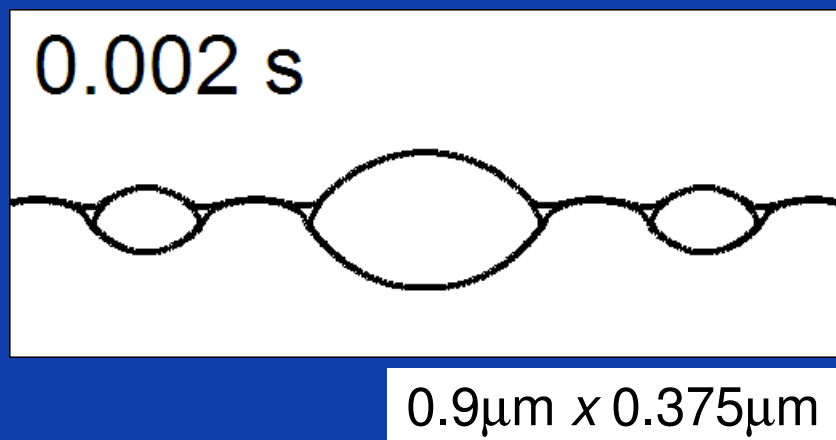
In collaboration with A. Miroux, E. Anselmino, S. van der Zwaag, T. U. Delft

Material properties at 723K

Grain boundary energy high angle	$\gamma_h = 0.324 \text{ J/m}^2$
Interfacial energy Al_6Mn precipitates	$\gamma_{pr} = 0.3 \text{ J/m}^2$
Mobility high angle grain boundary At solute content 0.3w% Mn	$M_h = 2.94 \cdot 10^{-11} \text{ m}^2\text{s/kg}$ (Miroux et al., Mater. Sci. Forum, 467-470, 393(2004))
Equilibrium composition of matrix	$c_{\text{Mn},eq} = 0.0524 \text{ w\% (0.02456 at\%)}$ (PhD thesis Lok 2005)
Actual composition of matrix (supersaturated)	$c_{\text{Mn}} = 0.3 \text{ w\% (0.1474 at\%)}$ (PhD thesis Lok 2005)
Mn diffusion in fcc Al	$D_{0,bulk} = 10^{-2} \text{ m}^2/\text{s}, Q_{bulk} = 211 \text{ kJ/mol}$ $\rightarrow D_{bulk} = 5.5973 \cdot 10^{-18} \text{ m}^2/\text{s}$
Pipe diffusion high angle boundaries, precipitate/matrix interface	$D_{0,p} = D_{0,bulk}, Q_p = 0.65Q_{bulk}$ $\rightarrow D_p = 1.2195 \cdot 10^{-12} \text{ m}^2/\text{s}$
Bulk energy density: $f^p = A^p(x - x^p_0)^2$	$A^m = 6 \cdot 10^{11}; x^m_0 = 0.000258$ $A^p = 6 \cdot 10^{12}; x^p_0 = 0.1429$

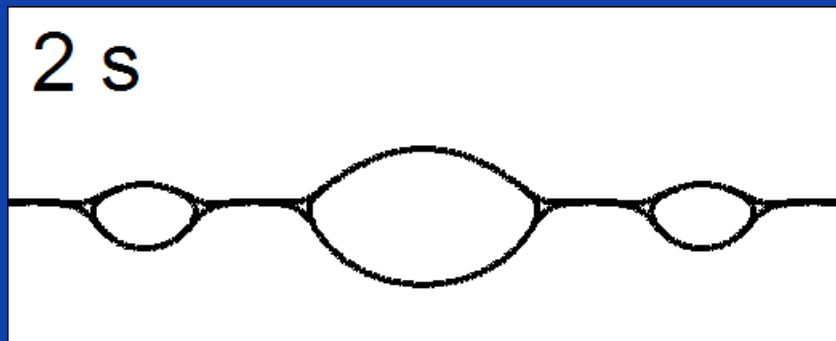
Precipitate coarsening and unpinning

- $P_D < P_{zs}$ ($P_D \approx P_{zs}$)
 - Pinning: $P_{zs}=3.6$ MPa
 - Rex: $P_D=3.1$ MPa
- Unpinning mainly through surface diffusion around precipitates



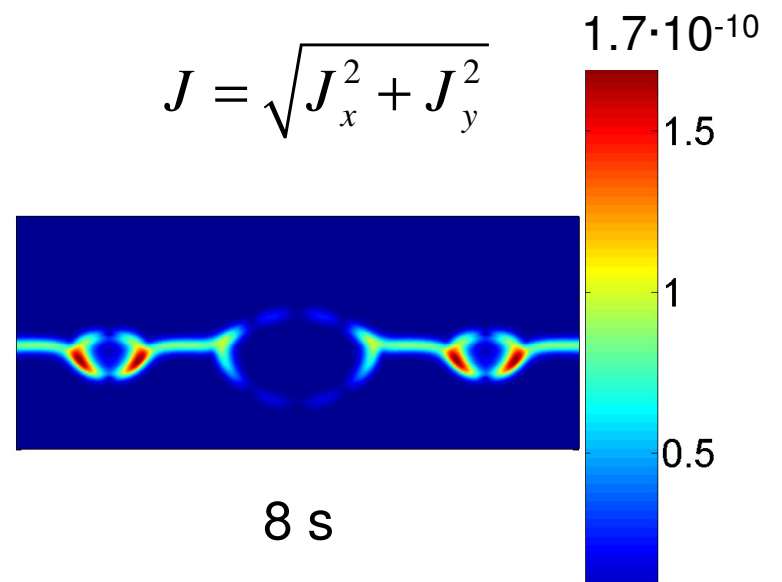
Precipitate coarsening and unpinning

- $P_D \lll P_{zs}$
 - Pinning: $P_{zs} = 3.6 \text{ MPa}$
 - $Rex: P_D = 1.1 \text{ MPa}$



$0.9\mu\text{m} \times 0.375\mu\text{m}$

- Unpinning through grain boundary diffusion

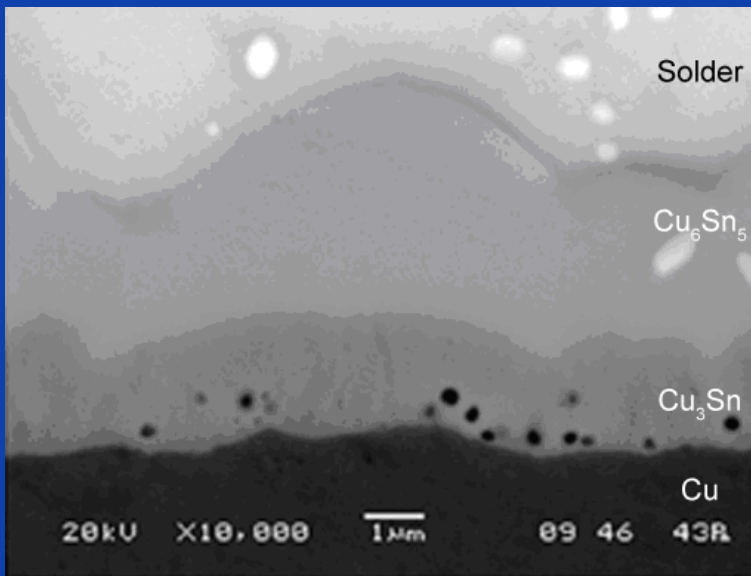


Examples of applications

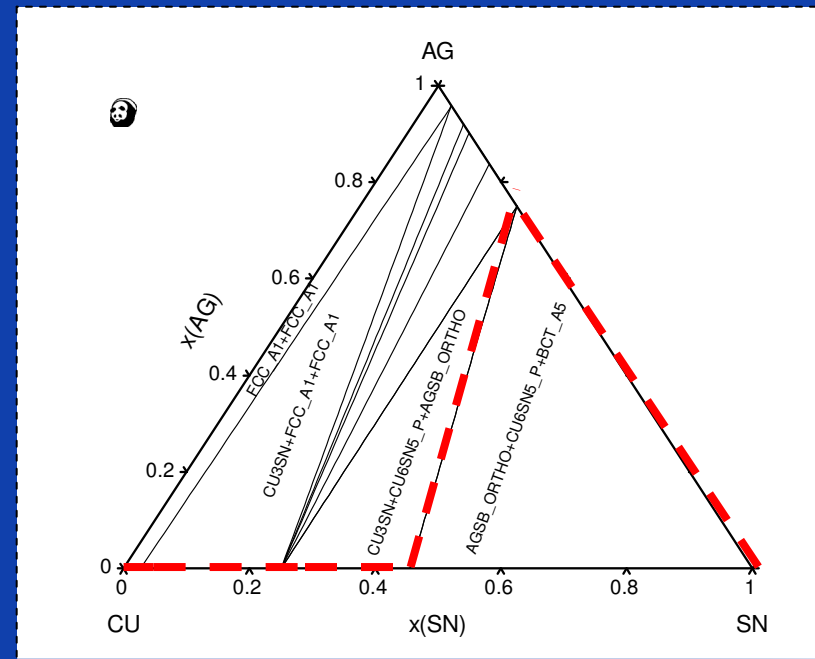
- Anisotropic grain growth
- Precipitates on grain boundaries
- Lead-free solder systems
- Solidification

Coarsening in Sn(-Ag)-Cu solder joints

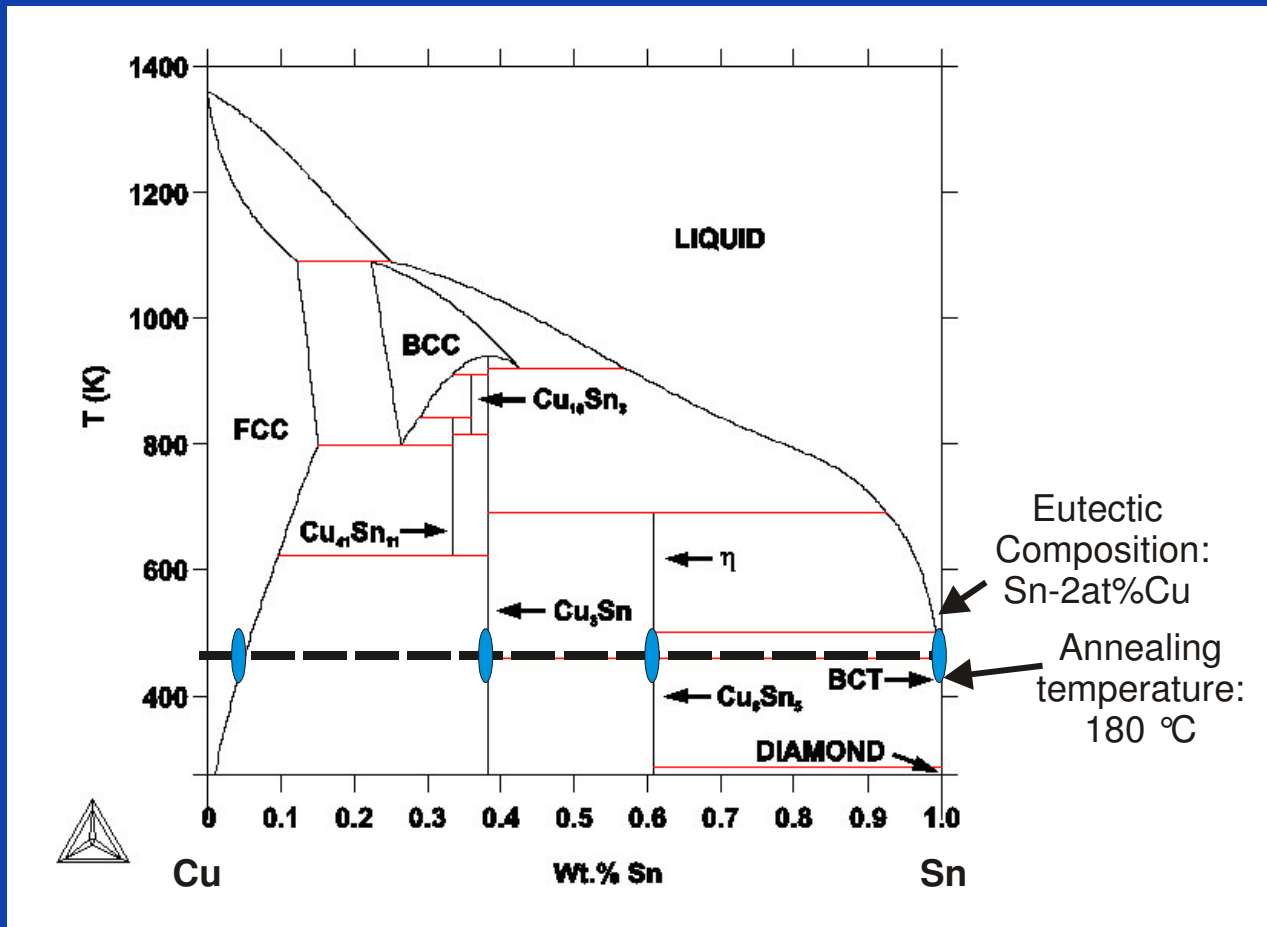
- COST MP-0602 (Advanced Solder Materials for High Temperature Application)
 - IMC formation and growth – precipitate growth – Kirkendal voids – stresses – grain boundary diffusion
 - CALPHAD description
 - Diffusion coefficients, growth coefficient for IMC-layers



SEM-image of Sn - 3.8Ag - 0.7 Cu alloy after annealing for 200h at 150 °C



- *Equilibrium compositions*



- *Interdiffusion coefficients*

$$D_{Sn}^{(Cu)} = 10^{-25}$$

$$D_{Sn}^{Cu_3Sn} = 5 \cdot 10^{-16} \text{ m}^2/\text{s}$$

$$D_{Sn}^{Cu_6Sn_5} = 10^{-15} \text{ m}^2/\text{s}$$

$$D_{Sn}^{(Sn)} = 10^{-12} \text{ m}^2/\text{s}$$

- *Interfacial energy*

$$\sigma_{gb} = 0.35 \text{ J/m}^2$$

Effect of precipitates in Sn-2at%Cu

- **Interdiffusion coefficients:**

$$D_{Sn}^{(Cu)} = 10^{-25}, 10^{-12} \text{ m}^2/\text{s}$$

$$D_{Sn}^{Cu_6Sn_5} = 10^{-16}, 10^{-13}, 10^{-12} \text{ m}^2/\text{s}$$

$$D_{Sn}^{(Sn)} = 10^{-12} \text{ m}^2/\text{s}$$

- **Interfacial energies:**

$$0.35 \text{ J/m}^2$$

- **Initial volume fraction precipitates:**

$$f_V = 0.04$$

- **Interfacial reactions are diffusion controlled**

- **Initial compositions**

Solder:

$$x_{Sn,0} = 0.98$$

(Sn)-matrix

$$x_{Sn} = 0.999$$

Cu₆Sn₅-precipitates

$$x_{Sn} = 0.4545$$

IMC layer

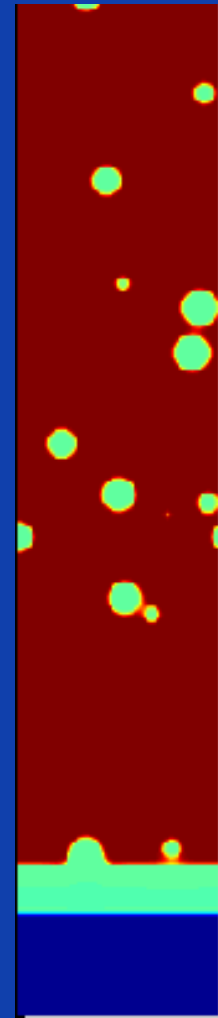


$$x_{Sn} = 0.4545$$

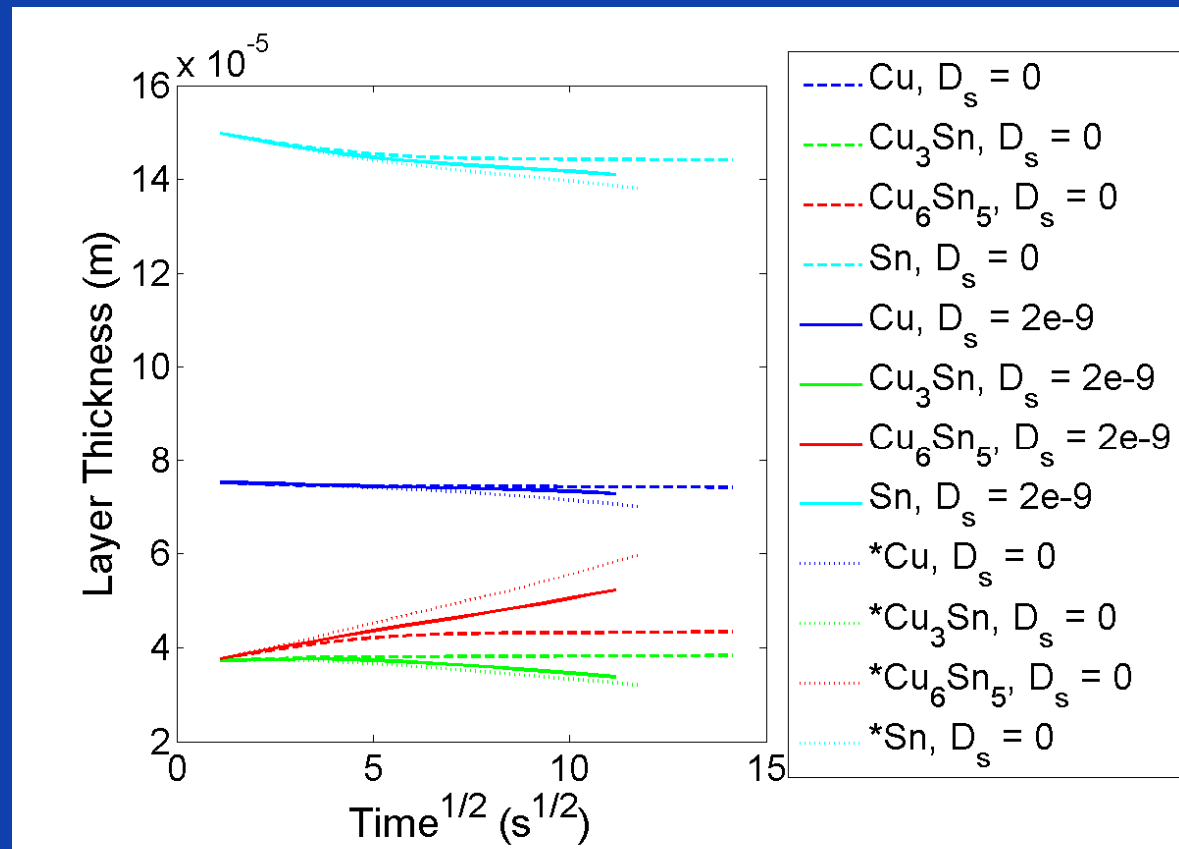
(Cu)-substrate

$$x_{Sn} = 0.001$$

• **System size: 0.1 μm x 0.5 μm**



Effect of grain boundary diffusion

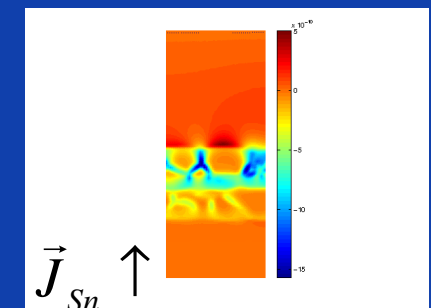
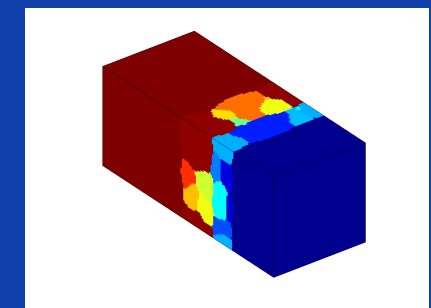


$$D_{Sn}^{(Cu)} = 2 \cdot 10^{-25}, * 2 \cdot 10^{-25} \text{ m}^2/\text{s}$$

$$D_{Sn}^{Cu_3Sn} = 2 \cdot 10^{-15}, * 2 \cdot 10^{-13} \text{ m}^2/\text{s}$$

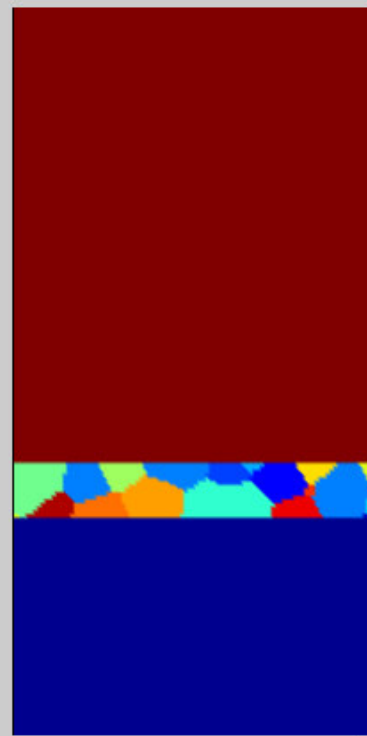
$$D_{Sn}^{Cu_6Sn_5} = 2 \cdot 10^{-15}, * 2 \cdot 10^{-13} \text{ m}^2/\text{s}$$

$$D_{Sn}^{(Sn)} = 2 \cdot 10^{-12}, * 2 \cdot 10^{-12} \text{ m}^2/\text{s}$$



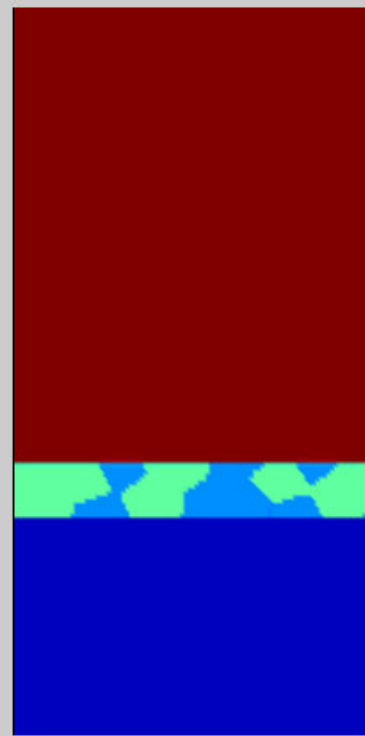
Growth behavior Cu₃Sn ?

Grain structure



time:0 sec

Composition: x_{Sn}



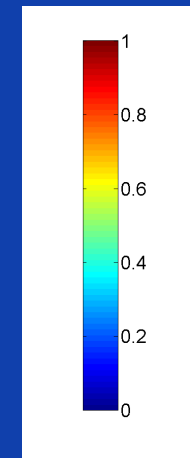
$$D_{Sn}^{(Cu)} = 2 \cdot 10^{-25} \text{ m}^2/\text{s}$$

$$D_{Sn}^{Cu3Sn} = 2 \cdot 10^{-15} \text{ m}^2/\text{s}$$

$$D_{Sn}^{Cu6Sn5} = 2 \cdot 10^{-15} \text{ m}^2/\text{s}$$

$$D_{Sn}^{(Sn)} = 2 \cdot 10^{-12} \text{ m}^2/\text{s}$$

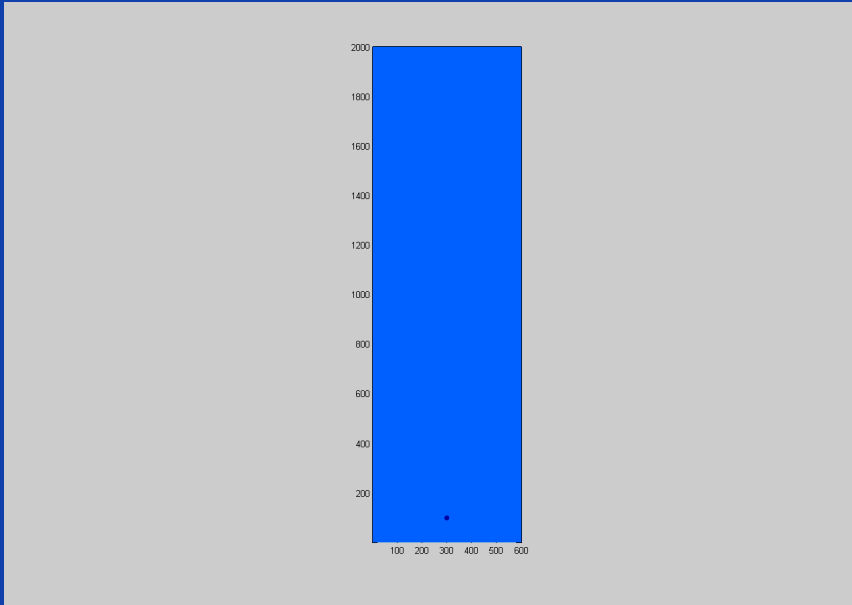
$$D_{Sn}^{surf} = 2 \cdot 10^{-12} \text{ m}^2/\text{s}$$



Examples of applications

- Anisotropic grain growth
- Zener pinning
- Coarsening of precipitates on grain boundaries
- Lead-free solder systems
- Solidification

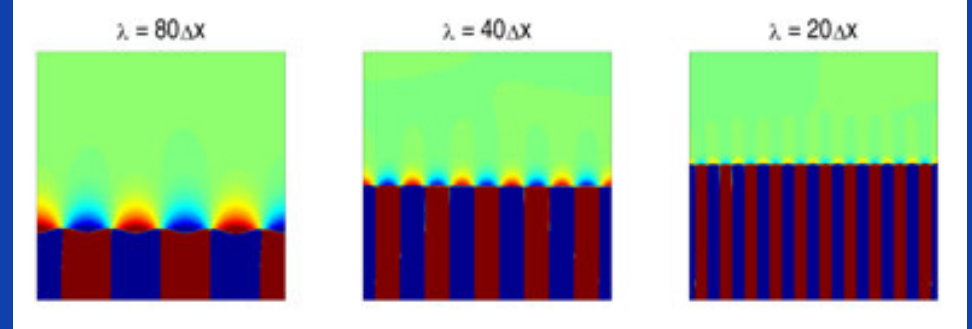
- *Dendritic growth*



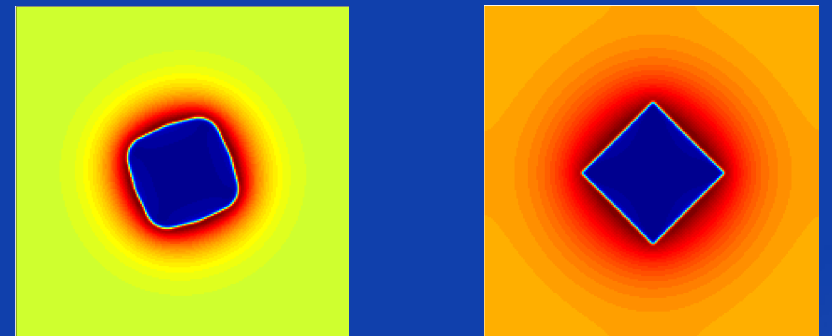
4-fold weak anisotropy in interface energy, Cu-Ni

J. Heulens, K.U. Leuven

- *Eutectic growth*



- *Faceted growth (strong anisotropy)*



4-fold anisotropy in interface energy

4-fold anisotropy in interface mobility

- Understanding microstructure evolution is important for material science, but processes can be very complex
 - Phase-field technique + other models and experimental input
- Principles phase-field modeling
 - Diffuse interface concept, conserved and non-conserved field variables
 - Evolution equations derived from a free energy functional
 - Quantitative aspects: Parameter choice + advanced implementation techniques
- Applications
 - Grain growth, recrystallization, coarsening, solidification, growth intermetallic phases, ...

Thank you for your attention ! Questions ?

- **Acknowledgements**
 - Research Foundation - Flanders (FWO-Vlaanderen)
 - Flemish Supercomputing Center (VSC)
- More information on *<http://nele.studentenweb.org>*